Catalytic Pyrolysis of Hemicellulose to Produce Aromatic Hydrocarbons

Yi Yang, Zhongyang Luo,* Simin Li, Kongyu Lu, and Wenbo Wang

Catalytic fast pyrolysis of hemicellulose with zeolite catalysts is a promising method to produce aromatic hydrocarbons (Carlson *et al.* 2009). In this paper, the behavior of hemicellulose catalytic pyrolysis with HZSM-5 (with three different silica to alumina ratio, 23, 50, 80), HY, and Hβ was studied. Pyrolysis vapor was separated into non-condensable vapors and condensable fractions. The fractions were qualified and quantified by a gas chromatography / flame ionization detector (GC/FID) system and a gas chromatography / mass spectrometer (GC/MS) system, respectively. The influences of catalysts and pyrolysis parameters were studied. Among the catalysts, HZSM-5(23) provided the desired acidity and shape selectivity for aromatic hydrocarbon production. A higher catalyst to hemicellulose ratio (CHR) and higher heating rate resulted in a higher aromatic hydrocarbon yield. The most suitable pyrolysis temperature for hemicellulose with HZSM-5 was 650 °C. During catalytic pyrolysis, thermal decomposition products underwent deoxygenation reactions promoted by the acid sites on the zeolite. The C2-C4 deoxygenated products produced monocyclic aromatic hydrocarbons (MAH) by shape-selective catalysis reactions in zeolite pores. With higher temperatures and higher residence times, monocyclic aromatic hydrocarbons facilitated cyclization reactions with C2-C4 deoxygenated products, thereby forming polycyclic aromatic hydrocarbons (PAH).

*Contact information: State Key Laboratory of Clean Energy Utilization, Zhejiang University, Hangzhou 310027, P.R. China; *Corresponding author: zyluo@zju.edu.cn*

INTRODUCTION

Benzene, toluene, ethyl benzene, and xylenes (BTEX), which are four important monocyclic aromatic hydrocarbons (MAH), are petrochemical materials used to manufacture many organic chemicals, plastic resins, synthetic fibers, solvents, and plasticizers. Naphthalene and anthracene, two important polycyclic aromatic hydrocarbons (PAH), are used as additives to jet fuel. Currently, MAH and PAH are mainly obtained from fossil petroleum. Catalytic pyrolysis of lignocellulosic biomass with some zeolite catalysts is a renewable approach to produce aromatic hydrocarbons (Zheng *et al.* 2017; Wang *et al.* 2018).

Some chemicals can be obtained in large quantities from plant biomass, including lignin, cellulose, and hemicellulose. Biomass pyrolysis produces non-condensable gas, condensable fractions (bio-oil), char, and coke. However, the bio-oil produced by non-catalytic pyrolysis mainly contains acids, furans, ketones, phenols, sugars, and some other oxygenates. Only a few aromatic hydrocarbons can be produced without a catalyst. Comparatively, catalytic fast pyrolysis of biomass with zeolite catalysts is a promising approach to produce aromatic hydrocarbons. Cellulose and hemicellulose produce more

bioresources.com

aromatic hydrocarbons than lignin (Shao *et al.* 2017). Cellulose and hemicellulose both consist of sugar monomers (Jun *et al.* 2004; Mullen and Boateng 2010; Wang *et al.* 2014; Kim *et al.* 2015). The difference is that cellulose only contains anhydrous glucose, while hemicellose includes xylan, glucuronoxylan, arabinoxylan, glucomannan, and xyloglucan. As a result, the reactions and products in catalytic pyrolysis of hemicellulose are more complicated. Moreover, considering the pretreatment of wood chips in kraft pulping process can obtain a certain purity of hemicellulose as the raw material for catalytic pyrolysis, kraft pulping can also be combined with hemicellulose catalytic pyrolysis industry to obtain important industrial raw materials.

In this case, xylan was used as a model compound to pyrolyse with HZSM-5 (with three different silica to alumina ratio, 23, 50, 80), HY, and Hβ. Non-condensable vapors and condensable fractions were qualified and quantified by a gas chromatography flame ionization detector (GC/FID) and gas chromatography mass spectrometer (GC/MS), respectively. The influence of catalysts and pyrolysis parameters were studied on this work.

EXPERIMENTAL

Feedstock

Xylan is commonly used as the model compound of hemicellulose (Giudicianni *et al.* 2013; Stefanidis *et al.* 2014). In this study, xylan powder (Sigma Aldrich, St. Louis, MO, USA) from corn cob was used as pyrolysis feedstock. Its appearance was white to yellow. Prior to the experiment, xylan particles were dried at 105 °C to remove moisture.

Catalysts Preparation and Characterization

HZSM-5(23), HZSM-5(50), HZSM-5(80), HY, and Hβ, purchased from Tianjing Nankai catalyst company, were used as catalysts in the pyrolysis experiments. Prior to all experiments and characterization, all of the catalysts were dried and degassed at 120 °C overnight.

To obtain the surface area and pore size distribution of the catalysts, nitrogen adsorption and desorption isotherms were acquired from a chemical station (Micromeritics ASAP-2010). All samples were pretreated in vacuum at 220 °C for 24 h before physisorption. The surface areas were derived from a standard Brunauer–Emmett–Teller (BET) equation. The average pore diameters were calculated using Barret–Joyner–Halenda (BJH) analysis (Zhang *et al.* 2012).

To compare the acidity of HZSM-5 with different silicon to aluminum ratios (SAR), temperature programmed desorption of ammonia (NH_3-TPD) was performed in an AutoChem II 2910 (Micromeritics, Norcross, GA, USA) device with mass spectrometry (MS). In a typical run, after degassing at 550 °C in a flow of He (50 mL/min), 0.1 g of catalyst was exposed in a flow of NH_3 (15% NH_3 + 85% He, 50 mL/min) at 60 °C for 1 h. To remove the physically absorbed NH_3, the catalyst sample was flushed by He (50 mL/min) at 100 °C for 2 h. The sample was heated to 700 °C (10 °C/min). The amount of chemically adsorbed NH_3 was recorded by MS (Dang *et al.* 2013).

Catalytic Pyrolysis Experimental Procedure and Products Analysis
Catalytic pyrolysis of hemicellulose

The experiments were carried out with a microscale pyrolysis unit, CDS Pyroprobe 5250 (CDS Analytical Inc., Oxford, PA, USA), which can adjust the pyrolysis parameters

(heating rate, pyrolysis temperature, residence time). The structure of the pyroprobe is shown in Fig. 1. For typical pyrolysis experiments, about 0.50 mg of xylan was placed between quartz wool in a quartz tube. For catalytic pyrolysis experiments, the catalysts and xylan were premixed with a 5:1 mass ratio. After that, about 3.0 mg of the mixture was placed between quartz wool to ensure approximately 0.5 mg xylan would be pyrolysed. For each sample, five or more replicates were run. Pyrolysis proceeded by setting the pyroprobe at 600 °C at a heating rate of 1000 K/s. After pyrolysis, the product vapor of hemicellulose diffused and reacted with the presence of catalysts. To ensure that all the reactions occurred thoroughly, a hold time of 30 s was set. During the reaction, a stream of 20 mL/min of helium was used as a carrier gas to purge both non-condensable gases and condensable fractions out. A trap setting at 40 °C was designed to separate non-condensable gases and condensable fractions. Non-condensable gases were purged directly through the trap to a GC-FID for separation and identification, while condensable fractions were captured by the trap. The trap was heated, and condensable fractions were purged into the GC-MS by carrier gas for separation and identification.
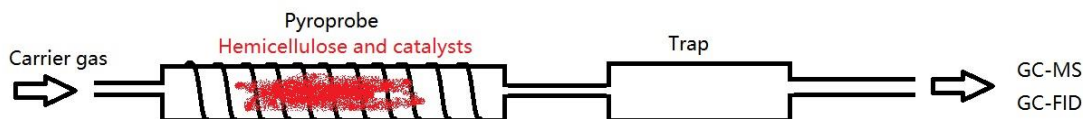

Fig. 1. Structure of CDS 5250 pyroprobe

Condensable fractions

Condensable fractions were separated and identified by a GC-MS (Thermo Fisher TRACE2000-DSQII, Waltham, MA, USA) with an HP-5 column (Agilent, Santa Clara, CA, USA). The detailed temperature control program was described previously (Dang *et al.* 2013).

The C6-C10+PAH was identified and quantified (C6-benzene; C7-toluene; C8-xylene, ethyl benzene; C9-trimethyl benzene, methyl ethyl benzene, indane, indene; C10+PAH-naphthalene, methylnaphthalene, anthracene, phenanthrene). The products were identified to compare the mass spectra of the peaks with the NIST library. The pure compounds of aromatic hydrocarbons mentioned above (Sigma Aldrich) were used to do the quantification by external standards with a five-point calibration curve.

Non-condensable gases

Non-condensable gases were separated and identified using a 7890A GC-FID device (Agilent). The gases were separated in the column. The alkanes and alkenes from the pyrolysis reactions and catalytic reactions were detected by FID. The pure standard gases were used to confirm all the alkanes and alkenes. Quantification of alkanes and alkenes was performed using external standards with a five-point calibration curve.

RESULTS AND DISCUSSION

Catalyst Properties

Table 1 shows the comparison of nitrogen adsorption/desorption properties of the catalysts used in this paper. Like other typical microporous catalysts, HZSM-5 had an average pore size from 0.498 nm to 0.510 nm with different SAR. The BET surface area

and the pore volume of different HZSM-5 decreased from 357.7 m^2/g to 259.7 m^2/g and 0.184 cm^3/g to 0.132 cm^3/g, respectively, with the increase of SAR. This result implied that the reaction activities of HZSM-5 decreased. HY had a similar pore size as HZSM-5 of 0.511 nm, a larger surface area of 660.4 m^2/g, and a larger pore volume of 0.338 cm^3/g. Hβ had the largest pore size among all five zeolite catalysts.

Table 1. Structure Properties of the Catalysts by Nitrogen Adsorption/Desorption

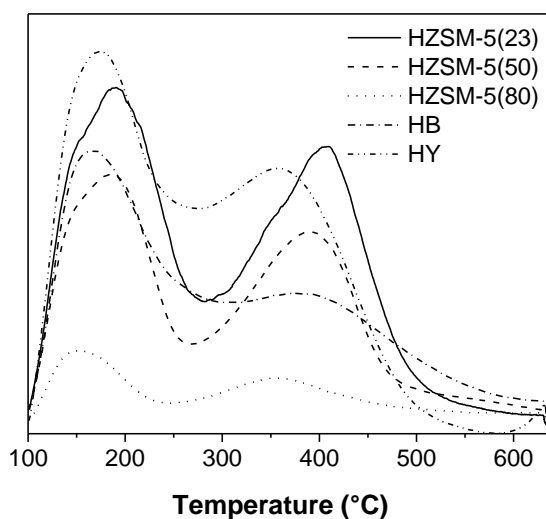| Catalyst	BET Surface Area(m^2/g)	Pore Size (nm)	Pore Volume (cm^3/g)
HZSM-5(23)	358	0.501	0.184
HZSM-5(50)	315	0.498	0.157
HZSM-5(80)	260	0.510	0.132
HY	660	0.511	0.338
Hβ	527	0.767	0.405

Fig. 2. NH_3 desorption amount of catalysts by NH_3-TPD

Table 2. Relative Total Acidity of Catalysts from NH_3-TPD

Catalyst	Total Acidity (mmol NH_3/g)
HZSM-5(23)	0.270
HZSM-5(50)	0.200
HZSM-5(80)	0.066
HY	0.283
Hβ	0.213

Figure 2 and Table 2 shows the NH_3 desorption amounts of HZSM-5 catalysts with different SAR in NH_3-TPD. The NH_3 desorption curves illustrated the strength and amount of acid. The curves of three HZSM-5 each had a peak located from 150 °C to 200 °C, which represented weak acid sites. Another peak related to strong acid sites occurred around 370 °C. Both peaks drifted to higher temperatures with lower SAR, which indicated that the strength of acid sites increased with the decease of SAR. Additionally, with the decrease of SAR, the total acidity increased significantly, which demonstrated that the amount of acid sites increased. For HY and Hβ, the curves had two desorption peaks. One of them

was about 150 °C, while the other was about 370 °C. The total acidity of HY was slightly higher than HZSM-5(23), while Hβ's total acidity was between HZSM-5(23) and HZSM-5(50).

Influence of Catalyst

Influence of different catalysts

To compare the different catalysts, 0.50 mg of xylan was mixed with five different catalysts (2.50 mg). The mixture was pyrolyzed at 600 °C at a heating rate of 10,000 K/s. HZSM-5, HY, and Hβ are zeolites are based on SiO_2 and Al_2O_3 structures, which results in strong acid sites and high activity in the deoxygenation reaction. As shown in Fig. 3, the deoxygenation reaction produced mainly alkenes in non-condensable gas. Ethylene and propylene had a higher yield in HZSM-5 (23, 50) due to the deoxygenation reaction. HY tended not to break the C-C bond, which resulted in a higher selectivity of propylene and butylene when compare to the rest of the catalysts. Comparatively, HZSM-5(23), which had the strongest acid sites among three HZSM-5 type catalysts, produced the most alkanes and alkenes. Hβ tended to produce more alkane.
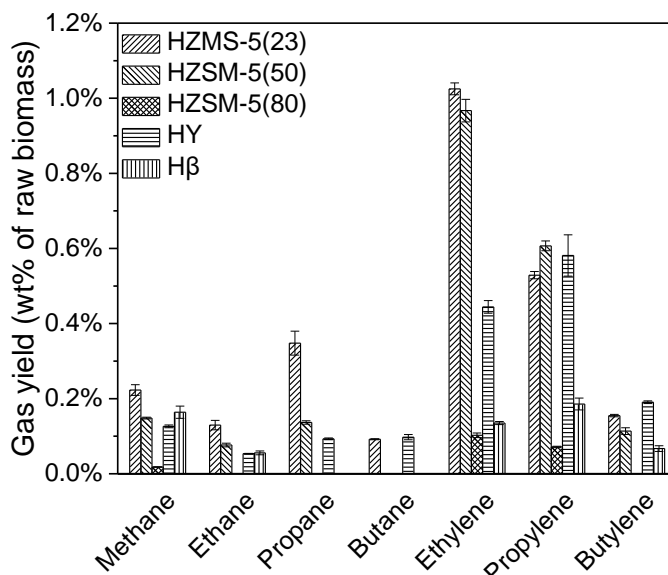

Fig. 3. None-condensable gases from catalytic pyrolysis of hemicellulose with different catalysts

As can been seen in Table 3, non-catalytic of hemicellulose mainly produced low molecular weight oxygenates, furans, phenols, and sugars. Only 1.75% (peak area) of naphthalene was obtained from non-catalytic pyrolysis. On the contrary, catalytic pyrolysis with HZSM-5(23) produced mainly MAHs and PAHs.

According to Fig. 4, all five catalysts produced different amounts of MAH and PAH in condensable fractions. To compare the catalysts, all the MAH and PAH detected in condensable fractions were identified and quantified by external standards. HY and Hβ had a lower reaction activity for aromatic hydrocarbon production. From C7-C9, HY had the lowest yield. Due to its 0.767 nm pore size, Hβ mainly produced C10+PAH. HZSM-5 (23 and 50) achieved almost the same aromatic hydrocarbon yield, which was a much higher yield than HZSM-5 (80), due to both its strong acid sites and its high selectivity in the aromatic production reaction.

bioresources.com

Table 3. Comparison between Non-catalytic and Catalytic Pyrolysis

Category	Chemical	Peak Area of GC-MS	
		Direct Pyrolysis	Catalytic Pyrolysis with HZSM-5(23)
Low molecular weight oxygenates	1-Propen-2-ol, acetate	1.46%	
	Acetic acid	1.18%	
Total		2.64%	0.00%
Furans	3-Furaldehyde	33.73%	1.70%
	2-Furaldehyde	37.51%	1.00%
	2-Hydroxymethylfuran	1.57%	
	3-Methyl-1,2-cyclopentanedione	0.97%	
	3-Hydroxymethylfuran	3.59%	
Total		77.37%	2.70%
Phenols	4-Ethoxyphenol	3.66%	
	3-Methoxyphenol	1.11%	
	Catechol	1.09%	
	Phenol		0.61%
Total		5.87%	0.61%
Sugars	Xylose	8.20%	
	d-Arabinose	1.83%	
	lactose	1.34%	
Total		11.36%	0.00%
MAHs	Benzene		2.42%
	Toluene		16.49%
	Xylene		10.62%
	Ethylbenzene		0.59%
	Trimethylbenzene		1.49%
	Indane		0.69%
	Indene		1.97%
Total		0.00%	34.26%
PAHs	Naphthalene	1.75%	27.64%
	2-Methylnaphthalene		29.11%
	1-Methylnaphthalene		1.89%
	2-Vinylnaphthalene		0.54%
	Anthracene		1.69%
Total		1.75%	60.87%

Comparatively, HZSM-5 (50) produced the most MAH and PAH among all five catalysts. Figure 5 shows that HZSM-5 series catalysts produced lot of MAHs such as C6, C7, and C8. When the carbon chain continued to increase, HZSM-5 tended to produce more C10+PAH than C9. On the contrary, Hβ might have had the potential to produce more C10+PAH, since it had a higher C10+PAH selectivity and lower C6-C8 selectivity than the HZSM-5 series catalysts.
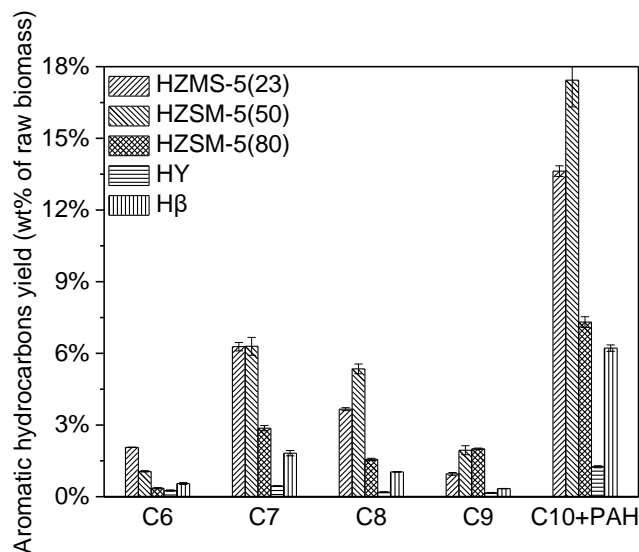
Fig. 4. Aromatic hydrocarbons from catalytic pyrolysis of hemicellulose with different catalysts (C6-benzene; C7-toluene; C8-xylene, ethyl benzene; C9-trimethyl benzene, methyl ethyl benzene, indane, indene; C10+PAH-naphthalene, methylnaphthalene, anthracene, phenanthrene)
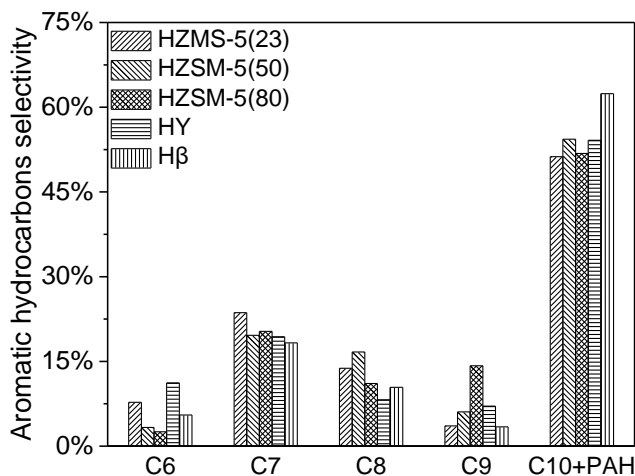

Fig. 5. Selectivity of aromatic hydrocarbons from catalytic pyrolysis of hemicellulose with different catalysts

Both HZSM-5 (23) and HZSM-5(50) were able to obtain high yield of MAHs and PAHs in catalytic pyrolysis of hemicellulose. HZSM-5 (23) had higher yield of alkanes and olefins. Further conversion of these alkanes and olefins under suitable conditions was able to produce more monocyclic aromatic hydrocarbons. HZSM-5 (50) had higher yields of MAHs and PAHs, but HZSM-5 (23) has higher selectivity for MAHs. HZSM-5(50) tended to produce more PAHs, and the increasing selectivity of PAHs would lead to more carbon deposition and deactivation of catalysts. Therefore, compared although the yield of monocyclic and polycyclic aromatic hydrocarbons was slightly lower than that of HZSM-5 (50), HZSM-5 (23) had advantages in other aspects.

bioresources.com

Table 4. Comparison between HZSM-5 (23) and HZSM-5 (50)

Yield	HZMS-5(23)	HZSM-5(50)	Selectivity	HZMS-5(23)	HZSM-5(50)
Alkanes	0.79%	0.36%			
Alkenes	1.71%	1.69%			
MAHs	11.29%	14.65%	MAHs	48.76%	45.67%
PAHs	13.63%	17.43%	PAHs	51.24%	54.33%

Influence of catalyst to hemicellulose ratio (CHR)

In this section, 0.50 mg of xylan was mixed with HZSM-5(23) with three different ratios, 5:1, 1:1, and 1:5. The mixture was pyrolyzed at 600 °C with a heating rate of 10,000 K/s and a residence time of 30 s.

The decrease of CHR resulted in less deoxygenation reactions, and less alkanes and alkenes were obtained (Fig. 6). At the same time, fewer aromatic hydrocarbons were acquired (Fig. 7), and the aromatic hydrocarbon yield decreased. The decreasing yield proved that unique pore structures from zeolite catalysts are necessarily in the production of aromatic hydrocarbons. However, MAHs and alkenes are thought to be precursors of C10+PAH. With a lower CHR, the unstable intermediate products were more dispersed. Thus, the intermediate products were less likely to react with each other to increase the carbon chain. This implied that increasing the carbon chain became more difficult with the decrease of CLR. As shown in Fig. 8, the selectivity peak shifted from C10+PAH to C8 with the decrease of CHR. The ratio that had the highest selectivity on C10+PAH was 5:1, while 1:1 and 1:5 had the highest on C9 and C7, respectively.
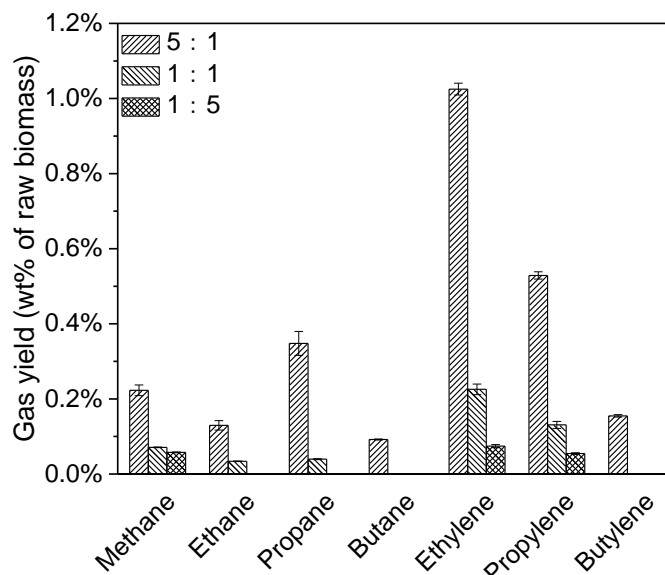
Fig. 6. Non-condensable gases from catalytic pyrolysis of hemicelluloses with different CHR
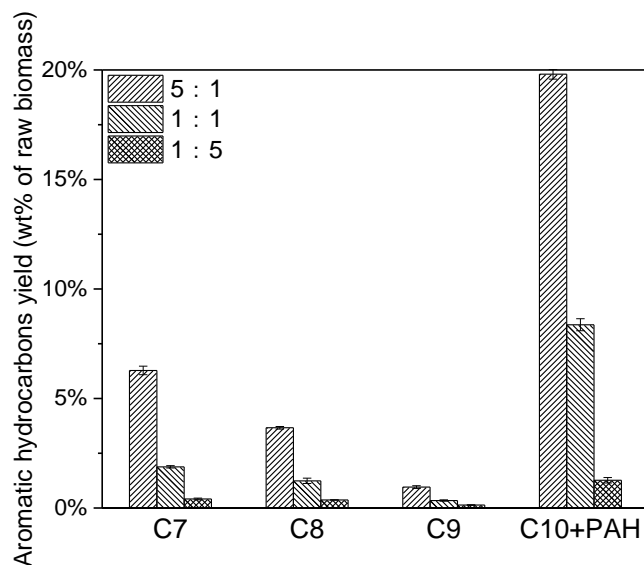
Fig. 7. Aromatic hydrocarbons from catalytic pyrolysis of hemicellulose with different CHR
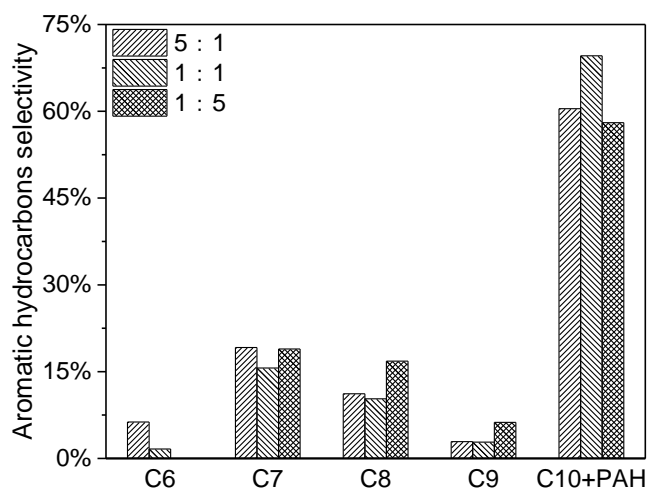

Fig. 8. Selectivity of aromatic hydrocarbons from catalytic pyrolysis of hemicellulose with different CHR

Influence of Pyrolysis Parameter

Influence of pyrolysis temperature

In this section, 0.50 mg of xylan was mixed with 2.50 mg of HZSM-5 (Sun *et al.* 2014). The mixture was pyrolyzed with a heating rate of 10,000 K/s at different temperatures ranging from 450 °C to 700 °C. As shown in Fig. 9, with a higher pyrolysis temperature, catalytic pyrolysis tended to produce more alkanes and alkenes due to a severe thermal decomposition reaction.
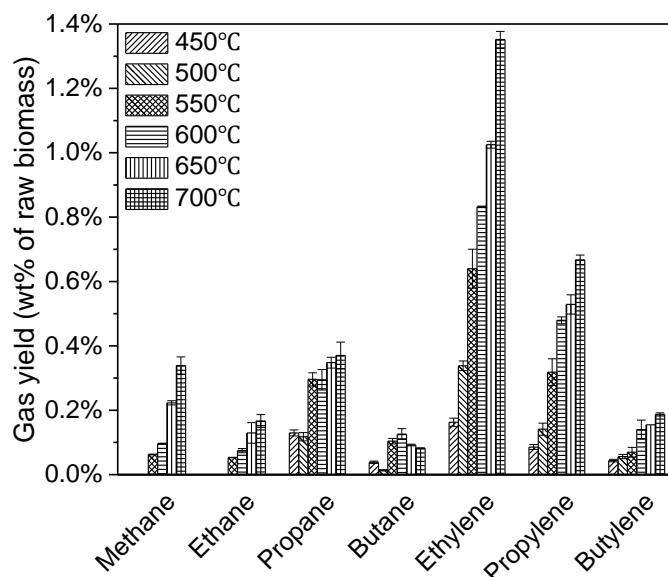
Fig. 9. Non-condensable gases from catalytic pyrolysis of hemicellulose with different pyrolysis temperatures

The influences of pyrolysis temperature on condensable fractions are shown in Fig. 10. For all C6 to C10 aromatic hydrocarbons, the yield increased from 450 °C to 650 °C, then decreased after 650 °C.
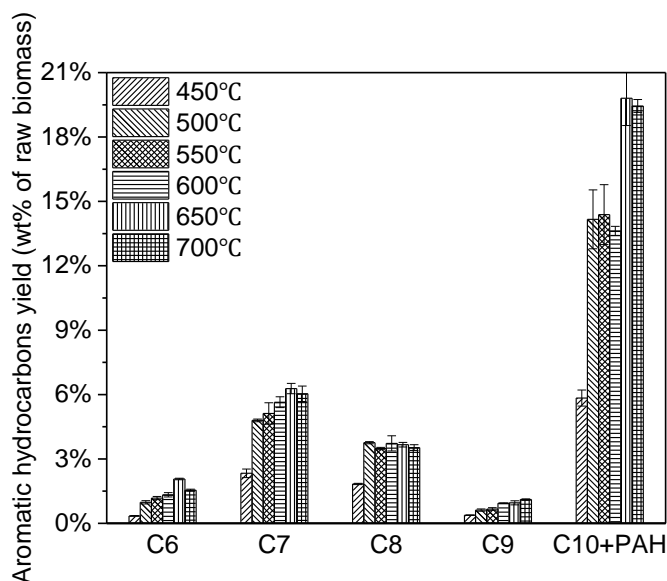

Fig. 10. Aromatic hydrocarbons from catalytic pyrolysis of hemicellulose with different pyrolysis temperatures

As mentioned above, during the catalytic pyrolysis process, hemicellulose was thermally decomposed to produce pyrolysis vapor. With a higher temperature, the feedstock was decomposed more severely. Thus, more intermediate products would undergo a deoxygenation reaction, and more aromatic hydrocarbons would be generated.

When the temperature rose higher than 650 °C, it caused the second decomposition reaction of intermediate products (acid, furan, phenol, and sugar) and final products (MAH and PAH) to produce C1-C2 alkanes, alkenes, and coke. However, at 650 °C, 7.65 wt% of aromatic hydrocarbon was produced.
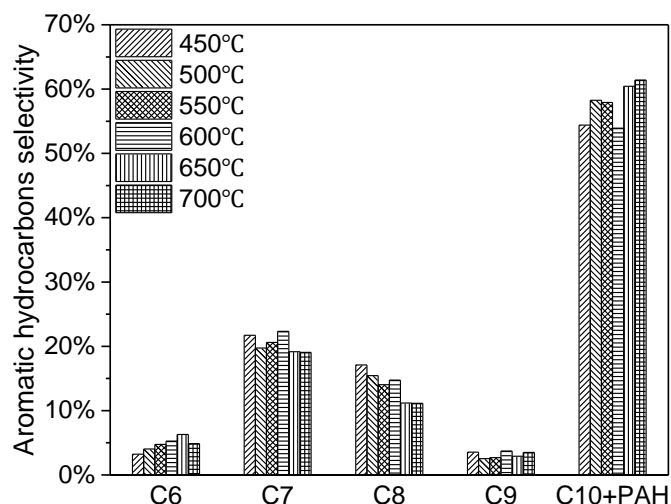

Fig. 11. Selectivity of aromatic hydrocarbons from catalytic pyrolysis of hemicellulose with different pyrolysis temperatures

Influence of heating rate

To compare the influence of the heating rate, 0.5 mg of xylan was mixed with 2.5 mg of HZSM-5 (23). The mixture was pyrolyzed using the Pyroprobe at 600 °C with different heating rates that ranged from 10 K/s to 10,000 K/s.
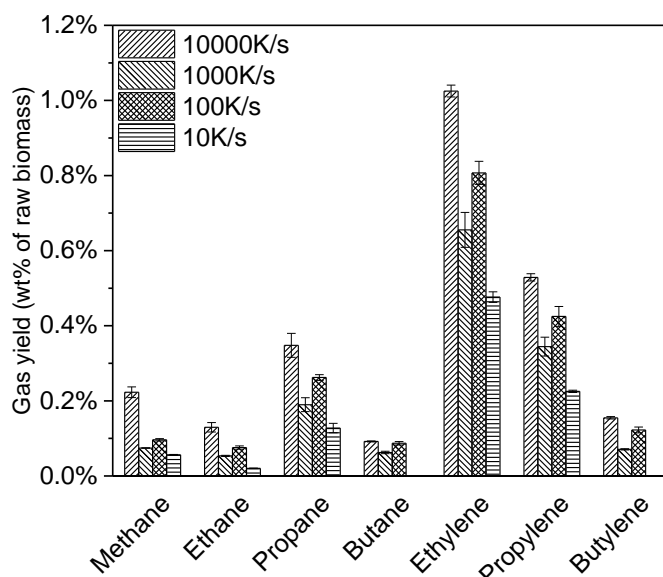

Fig. 12. Non-condensable gases from catalytic pyrolysis of hemicellulose with different heating rates

After achieving 600 °C, the pyrolysis system was held for 30 s for reaction. For example, at a heating rate of 10K/s the pyroprobe was heated up from 20 °C (room temperature) to 600 °C, which took around 58 s. Considering that the system was held for another 30 s, the whole reaction time was 88 s. For 100 K/s and 1000 K/s, the real residence times were 35.8 s and 30.6 s, respectively.

As mentioned above, a higher heating rate resulted in an increase of pyrolysis vapor yield. The presence of more pyrolysis vapor generated more C6-C10 aromatic hydrocarbons as well as C1-C4 alkanes and alkenes. The results are shown in Fig. 13.
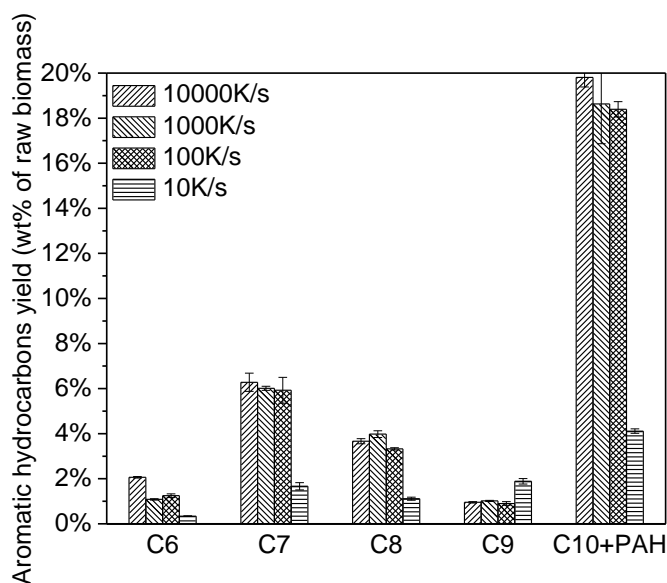

Fig. 13. Aromatic hydrocarbons from catalytic pyrolysis of hemicellulose with different heating rates
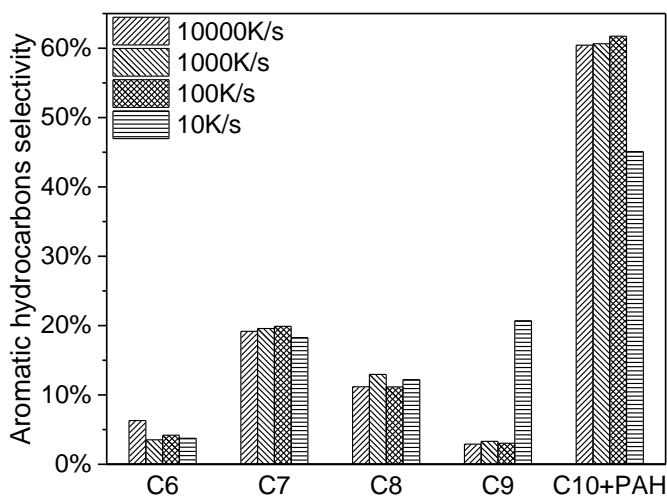

Fig. 14. Selectivity of aromatic hydrocarbons from catalytic pyrolysis of hemicellulose with different heating rates

The highest production for all C6-C10 aromatic hydrocarbons was achieved at a heating rate of 10,000 K/s. The yields of 10 k, 100 K/s, and 1000 K/s were similar, which might have been influenced by the "real residence time" issue.

Reaction Pathways to Aromatic Hydrocarbons

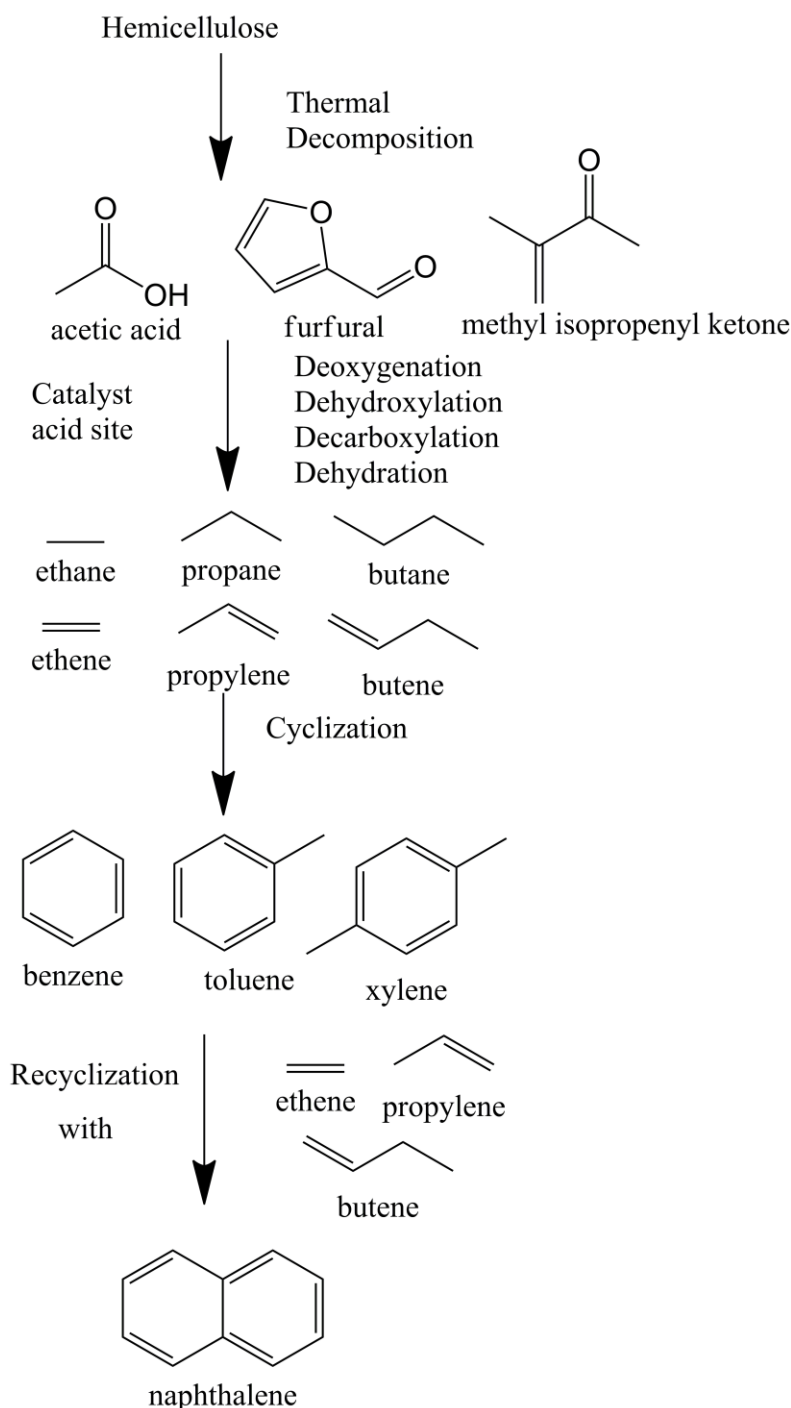As shown in Fig. 15, the hemicellulose catalytic pyrolysis process could be divided into two main steps.

Fig. 15. Reaction pathways of hemicellulose catalytic pyrolysis

bioresources.com

Firstly, hemicellulose isothermally decomposed into pyrolysis vapor, for instance, acids, aldehydes, furans, phenols, anhydrosugars, and so on (Nowakowski *et al.* 2010; Ben and Ragauskas 2013). The reaction mechanism of this step is consistent with the direct rapid pyrolysis of hemicellulose. Previous studies have shown that xylose undergoes isomerization to form other anhydrosugars during direct pyrolysis of hemicellulose (Zhou *et al.* 2017). Xylose and other anhydrosugars undergo ring opening and rearrangement reactions to form furans. In the ring opening and rearrangement reactions, decarbonylation and dehydration also take place, resulting in the formation of low molecular weight oxygenates such as acetic acid (Patwardhan *et al.* 2011; Shen *et al.* 2010; Wang *et al.* 2017). These pyrolysis products will then react with the catalyst in the second step. Under the action of HZSM-5 acidic site, a series of decarbonylation reactions will take place in the intermediate oxygenated products, resulting in more alkanes and olefins (Wang *et al.* 2014). In the process of converting methanol into aromatic hydrocarbons, olefin chain-growth reaction is widely recognized as an important approach to obtain aromatic hydrocarbons with HZSM-5 (Haw *et al.* 2003, Ilias and Bhan 2012). The above mentioned olefins exhibit similar carbon chain growth and cyclization with HZSM-5, resulting in MAHs production. Alkanes participate in the cyclization reaction and eventually form methyl or ethyl branched chains. Sun *et al.* (2014) and Huber and coworkers (Huber and Corma 2007; Huber *et al.* 2007; Foster *et al.* 2012) both emphasized the importance of a "hydrocarbon pool" in olefin to hydrocarbons and biomass catalytic fast pyrolysis respectively. MAHs will further react with olefins to form PAHs. As the pyrolysis temperature rises, this secondary cyclization reaction will intensify and eventually lead to carbon deposition. In this experiment, the yield of anthracene and phenanthrene kept increased further with the pyrolysis temperature rising to 700 °C, which is the main result of this secondary cyclization reaction.

CONCLUSIONS

1. The experiments showed that catalytic pyrolysis of hemicellulose with HZSM-5, HY, and Hβ was a promising way to obtain aromatic hydrocarbons. Among those catalysts, HZSM-5(23) provided the desired acidity and shape selectivity for aromatic hydrocarbon production. Higher CHR and a higher heating rate resulted in higher aromatic hydrocarbon yield. The most suitable pyrolysis temperature for hemicellulose with HZSM-5 was 650 °C.

2. In catalytic pyrolysis, thermal decomposition products underwent deoxygenation reaction by the acid site on zeolite. The C2-C4 deoxygenated products produced monocyclic aromatics by shape-selective catalysis in the zeolite pores. With higher temperatures and a higher residence time, monocyclic aromatic hydrocarbons would continue to undergo cyclization reactions with C2-C4 deoxygenated products to form PAH.

ACKNOWLEDGMENTS

REFERENCES CITED

Ben, H., and Ragauskas, A. J. (2013). "Influence of Si/Al ratio of ZSM-5 zeolite on the properties of lignin pyrolysis products," *ACS Sustainable Chemistry & Engineering* 1(3), 316-324. DOI: 10.1021/sc300074n

Carlson, T. R., Tompsett, G. A., Conner, W. C., and Huber, G. W. (2009). "Aromatic production from catalytic fast pyrolysis of biomass-derived feedstocks," *Topics in Catalysis* 52(3), 241-252. DOI: 10.1007/s11244-008-9160-6

Dang, Q., Luo, Z., Zhang, J., Wang, J., Chen, W., and Yang, Y. (2013). "Experimental study on bio-oil upgrading over Pt/SO$^{2-}_4$/ZrO$_2$/SBA – 15 catalyst in supercritical ethanol," *Fuel* 103, 683-692. DOI: 10.1016/j.fuel.2012.06.082

Foster, A. J., Jae, J., Cheng, Y.-T., Huber, G. W., and Lobo, R. F. (2012). "Optimizing the aromatic yield and distribution from catalytic fast pyrolysis of biomass over ZSM-5," *Applied Catalysis A: General* 423-424, 154-161. DOI: 10.1016/j.apcata.2012.02.030

Giudicianni, P., Cardone, G., and Ragucci, R. (2013). "Cellulose, hemicellulose and lignin slow steam pyrolysis: Thermal decomposition of biomass components mixtures," *Journal of Analytical and Applied Pyrolysis* 100, 213-222. DOI: 10.1016/j.jaap.2012.12.026

Haw, J. F., Song, W., Marcus, D. M., and Nicholas, J. B. (2003). "The mechanism of methanol to hydrocarbon catalysis," *Accounts of Chemical Research* 36(5), 317-326. DOI: 10.1021/ar020006o

Huber, G. W., and Corma, A. (2007). "Synergies between bio- and oil refineries for the production of fuels from biomass," *Angewandte Chemie International Edition* 46(38), 7184-7201. DOI: 10.1002/anie.200604504

Huber, G. W., O'Connor, P., and Corma, A. (2007). "Processing biomass in conventional oil refineries: Production of high quality diesel by hydrotreating vegetable oils in heavy vacuum oil mixtures," *Applied Catalysis A: General* 329, 120-129. DOI: 10.1016/j.apcata.2007.07.002

Ilias, S., and Bhan, A. (2012). "Mechanism of the catalytic conversion of methanol to hydrocarbons," *ACS Catalysis* 3(1), 18-31. DOI: 10.1021/cs3006583

Jun, K.-W., Roh, H.-S., Kim, K.-S., Ryu, J.-S., and Lee, K.-W. (2004). "Catalytic investigation for Fischer–Tropsch synthesis from bio-mass derived syngas," *Applied Catalysis A: General* 259(2), 221-226. DOI: 10.1016/j.apcata.2003.09.034

Kim, J.-Y., Lee, J. H., Park, J., Kim, J. K., An, D., Song, I. K., and Choi, J. W. (2015). "Catalytic pyrolysis of lignin over HZSM-5 catalysts: Effect of various parameters on the production of aromatic hydrocarbon," *Journal of Analytical and Applied Pyrolysis* 114, 273-280. DOI: 10.1016/j.jaap.2015.06.007

Mullen, C. A., and Boateng, A. A. (2010). "Catalytic pyrolysis-GC/MS of lignin from several sources," *Fuel Processing Technology* 91(11), 1446-1458. DOI: 10.1016/j.fuproc.2010.05.022

Nowakowski, D. J., Bridgwater, A. V., Elliott, D. C., Meier, D., and de Wild, P. (2010). "Lignin fast pyrolysis: Results from an international collaboration," *Journal of Analytical and Applied Pyrolysis* 88(1), 53-72. DOI: 10.1016/j.jaap.2010.02.009

Patwardhan, P. R., Brown, R. C., and Shanks, B. H. (2011). "Product distribution from the fast pyrolysis of hemicellulose," *ChemSusChem* 4(5), 636-643. DOI: 10.1002/cssc.201000425

Shao, L. P., You, T.T., Wang, C., Yang, G. H., Xu, F., and Lucia, L. (2017). "Catalytic

stepwise pyrolysis of technical lignin," *BioResources* 12(3), 4639-4651. DOI: 10.15376/biores.12.3.4639-4651

Stefanidis, S. D., Kalogiannis, K. G., Iliopoulou, E. F., Michailof, C. M., Pilavachi, P. A., and Lappas, A. A. (2014). "A study of lignocellulosic biomass pyrolysis via the pyrolysis of cellulose, hemicellulose and lignin," *Journal of Analytical and Applied Pyrolysis* 105, 143-150. DOI: 10.1016/j.jaap.2013.10.013

Sun, X. Y., Mueller, S., Liu, Y., Shi, H., Haller, G. L., Sanchez-Sanchez, M., van Veen, A. C., and Lercher, J. A. (2014). "On reaction pathways in the conversion of methanol to hydrocarbons on HZSM-5," *Journal of Catalysis* 317, 185-197. DOI:10.1016/j.jcat.2014.06.017

Wang, K., Kim, K. H., and Brown, R. C. (2014). "Catalytic pyrolysis of individual components of lignocellulosic biomass," *Green Chemistry* 16(2), 727-735. DOI: 10.1039/c3gc41288a

Wang, S., Dai, G., Yang, H., and Luo, Z. (2017). "Lignocellulosic biomass pyrolysis mechanism: A state-of-the-art review," *Progress in Energy and Combustion Science* 62: 33-86. DOI:10.1016/j.pecs.2017.05.004

Wang, X. Y., Wu, F., Li, C., Chen, M., and Wang, J. (2018). "High quality bio-oil production from catalytic microwave-assisted pyrolysis of pine sawdust," *BioResources* 13(3), 5479-5490. DOI:10.15376/biores.13.3.5479-5490

Zhang, J., Luo, Z., Dang, Q., Wang, J., and Chen, W. (2012). "Upgrading of bio-oil over bifunctional catalysts in supercritical monoalcohols," *Energy & Fuels* 26(5), 2990-2995. DOI: 10.1021/ef201934a

Zheng, Y. W., Tao, L., Yang, X., Huang, Y., Liu, C., Gu, J., and Zheng, Z. (2017). "Effect of acidity and manner of addition of HZSM-5 catalyst on the aromatic products during catalytic upgrading of biomass pyrolysis," *BioResources* 12(4), 8286-8305. DOI: 10.15376/biores.12.4.8286-8305

Zhou, X., Li, W., Mabon, R., and Broadbelt, L. J. (2017). "A critical review on hemicellulose pyrolysis," *Energy Technology* 5(1), 52-79. DOI: 10.1002/ente.201600327